Pharm Res (2015) 32:74–90
DOI 10.1007/s11095-014-1446-8

RESEARCH PAPER

Quantitative ADME Proteomics – CYP and UGT Enzymes in the Beagle Dog Liver and Intestine

Aki T. Heikkinen • Arno Friedlein • Mariette Matondo • Oliver J. D. Hatley • Aleksanteri Petsalo • Risto Juvonen • Aleksandra Galetin • Amin Rostami-Hodjegan • Ruedi Aebersold • Jens Lamerz • Tom Dunkley • Paul Cutler • Neil Parrott

Received: 7 May 2014 / Accepted: 2 July 2014 / Published online: 18 July 2014

ABSTRACT

Purpose Beagle dogs are used to study oral pharmacokinetics and guide development of drug formulations for human use. Since mechanistic insight into species differences is needed to translate findings in this species to human, abundances of cytochrome P450 (CYP) and uridine diphosphate glucuronosyltransferase (UGT) drug metabolizing enzymes have been quantified in dog liver and intestine.

Methods Abundances of enzymes were measured in Beagle dog intestine and liver using selected reaction monitoring mass spectrometry.

Results Seven and two CYPs were present in the liver and intestine, respectively. CYP3A12 was the most abundant CYP in both tissues. Seven UGT enzymes were quantified in the liver and seven in the intestine although UGT1A11 and UGT1A9 were present only in the intestine and UGT1A7 and UGT2B31 were found only in the liver. UGT1A11 and UGT1A2 were the most abundant UGTs in the intestine and UGT2B31 was the most abundant UGT in the liver. Summed abundance of UGT enzymes was similar to the sum of CYP enzymes in the liver whereas intestinal UGTs were up to four times more abundant than CYPs. The estimated coefficients of variation of abundance estimates in the livers of 14 donors were separated into biological and technical components which ranged from 14 to 49% and 20 to 39%, respectively.

Conclusions Abundances of canine CYP enzymes in liver and intestine have been confirmed in a larger number of dogs and UGT abundances have been quantified for the first time. The biological variability in hepatic CYPs and UGTs has also been estimated.

KEYWORDS Canine · Drug metabolism · Interspecies differences · Protein quantitation · *In vitro-in vivo* extrapolation

INTRODUCTION

Mass spectrometry based quantitative proteomics has been shown to be useful to measure the abundance of drug metabolizing enzymes and drug transporters in various human and animal tissues as well as in *in vitro* experimental systems derived from those tissues [1–3]. One motivation for such

Electronic supplementary material The online version of this article (doi:10.1007/s11095-014-1446-8) contains supplementary material, which is available to authorized users.

A. T. Heikkinen • A. Petsalo • R. Juvonen
School of Pharmacy, Faculty of Health Sciences, University of Eastern Finland, Kuopio, Finland

A. T. Heikkinen • A. Friedlein • J. Lamerz • T. Dunkley • P. Cutler • N. Parrott (✉)
Pharmaceutical Sciences, Pharmaceutical Research & Early Development, Roche Innovation Center Basel, Grenzacherstrasse 124, B70/R130, 4070 Basel, Switzerland
e-mail: neil_john.parrott@roche.com

M. Matondo • R. Aebersold
Department of Biology, Institute of Molecular Systems Biology, ETH Zurich, and Faculty of Science, University of Zurich, Zurich, Switzerland

O. J. D. Hatley • A. Galetin • A. Rostami-Hodjegan
Centre for Applied Pharmacokinetic Research, Manchester Pharmacy School, University of Manchester, Manchester M13 9PT, UK

O. J. D. Hatley • A. Rostami-Hodjegan
Simcyp Limited (a Certara Company), Blades Enterprise Centre, John Street, S2 4SU, Sheffield, UK

measurements is that enzyme/transporter activity *in vivo* and *in vitro* is believed to be proportional to enzyme/transporter abundance. Thus, abundance differences between an *in vitro* system and an intact tissue may be used as a scaling factor for *in vitro to in vivo* extrapolation (IVIVE) of activity [4, 5]. Furthermore, abundance measurements with associated variances may be applied for prediction of variability [6] and inter-population differences [7] in drug pharmacokinetics. Indeed, examples of utilization of mass spectrometry based quantitative proteomics data for IVIVE of drug metabolism and transport in physiologically based pharmacokinetic (PBPK) models have recently appeared [8–10].

PBPK models are a powerful tool for integration of quantitative data on different mechanisms affecting pharmacokinetics (PK) and for prediction of PK in human and animal populations. One strategy for prediction of human PK holds that confidence in predictions is improved by first building models for animal species and verifying them against *in vivo* observations [11, 12]. This strategy has proven useful, but it relies on a good understanding of the species differences in the mechanisms affecting PK in all the species used. Moreover, beagle dogs are often used to test clinical formulations [13] and gain insights into the mechanisms of food effects [14] and when predicting human oral PK, PBPK modeling in the dog has been shown to be useful as a verification step [15–17]. Such translational use of PK in dog needs to account for species differences in intestinal physiology [18–20] and in the function of drug metabolizing enzymes [21, 22]. Thus, recently developed dog specific tools, including biorelevant canine intestinal fluids [23] and scaling factors for IVIVE of cytochrome P450 (CYP) mediated metabolism [9, 24] have strengthened the approach. However, many gaps still remain and so the current study was performed to expand on previous work supporting the physiological basis of PBPK models of dog. Specifically, the abundances of the 7 CYP enzymes studied earlier in four donors [24] have been measured in an additional 14 livers and 5 intestines. Additionally, abundances of 12 UGT enzymes have been studied in the same samples. Microsomes, a subcellular fraction which excludes the nuclear and cytosolic proteins of the cell and is thus enriched with proteins located at the endoplasmic reticulum is commonly used as an *in vitro* model for CYP and UGT mediated metabolism. Furthermore, IVIVE of metabolism from microsomes generally uses enzyme independent scaling factors [25], assuming that each enzyme is equally enriched in the microsomal fraction. To evaluate the validity of this assumption, quantitative data on enzyme concentrations in both tissue homogenate and corresponding microsomal samples has been analyzed to derive values for the enrichment of individual enzymes achieved by the cell fractionation step. Moreover, replication of liver tissue processing was performed to allow separation of the technical and the underlying biological variability of CYP and UGT enzyme abundance. The estimates of biological variability provide a basis for bottom-up predictions of variability in hepatic metabolism. Furthermore, quantification of individual UGT protein levels expands significantly our knowledge of the enzymes involved in dog intestinal and hepatic glucuronidation.

In addition to their value in prediction for human, understanding of the factors affecting PK in dogs is obviously valuable for veterinary drug development and exploration of drug metabolizing enzymes as a source of variability in canine pharmacokinetics has been recently advocated by the FDA [20, 26].

MATERIALS AND METHODS

Chemicals

Unless otherwise noted, all the chemicals were from commercial sources and were of analytical grade or better.

Biological Samples

Beagle dog necropsy was performed at F. Hoffmann-La Roche Ltd (Nutley, NJ) according to institutional guidelines in compliance with national and regional legislation. All the donors were non-naïve animals used for pharmacokinetic studies, but had not received any investigational compounds within the 6 months prior to necropsy. The ages and weights of the dogs ranged from 31 to 35 months and from 7 to 14 kg, respectively.

Liver samples weighing approximately 10 g were collected from 4 female and 10 male beagle dogs and were snap frozen with liquid nitrogen. The liver samples were stored at −80°C until further processing.

Intestinal tissue was collected from 3 female and 2 male beagle dogs. Small intestines were divided into 5 equal segments (median length 53 cm), and colon (median length 29 cm) collected as a separate anatomical segment at Roche (Nutley, NJ). Each segment was flushed with ice cold Dulbeccos Phosphate Buffered Saline, supplemented with glucose and sodium pyruvate (Lifetechnologies), and containing protease inhibitor cocktail (Sigma). The small intestine was divided into equal length segments, instead of anatomical division to duodenum, jejunum and ileum, in order to minimize the tissue handling times and protein degradation before washing the segments and addition of protease inhibitor. Segments were shipped overnight on wet ice in fresh flush solution to Bristol-Myers Squibb (Princeton, NJ) and were further processed within 10 h of arrival.

Liver Microsomal Preparation

In order to minimize protein degradation, all the tissue processing steps were done on ice. Liver tissue was thawed, divided into three equal size samples and the weight of each sample was recorded. Further tissue processing was conducted in triplicate from each donor.

The liver samples were chopped into small pieces with a scalpel and homogenized using Ultra-Turrax homogenizer for 10 s in 100 mM Tris–HCl buffer, pH 7.4, containing 1 mM K_2-EDTA (4 ml g^{-1} liver) and further homogenized by 10 passes in Potter Elvehjem rotating homogenizer. Liver homogenate was centrifuged at 10 000 g for 15 min at 4°C. The supernatant ('S9 fraction') was collected, weighed and centrifuged at 100 000 g for 60 min at 4°C. The supernatant (cytosolic fraction) and pellet (microsomal fraction) were separated and weighed. The microsomal fraction was re-homogenized with 10 passes in Potter Elvehjem homogenizer in 100 mM Tris–HCl buffer, pH 7.4, containing 1 mM K_2-EDTA and 20% glycerol (0.7 ml g^{-1} liver). During tissue processing, 2 ml samples were collected, weighed and aliquoted from tissue homogenate, S9, cytosol and microsomal fractions followed by measurement of protein concentration using Bicinchoninic acid Assay (Pierce Biotechnology, IL, USA). The samples were stored at −80°C until further use.

Intestinal Microsomal Preparation

Intestinal homogenates were collected and microsomes were prepared from all segments for 2 male and 2 female dogs, and, additionally, homogenate samples were collected from segments 1, 3, 5 and colon from 1 additional female dog. Intestinal microsome preparation was performed using an optimized method developed in the rat and modified for dog tissue (*Hatley OJD, Jones C, Galetin A & Rostami−Hodjegan A.* [*Manuscript in preparation*]). In brief, on transfer to the lab, intestines were flushed with ice cold Solution A, pH7.4, consisting of Dulbeccos phosphate buffered saline buffer without Ca2+ and Mg2+ (used in all subsequent microsome preparation buffers), 27 mM sodium citrate monobasic, 0.5 mM dithiothreitol, and protease inhibitor cocktail. Intestines were then filled with solution A re-clamped and incubated on ice in Solution A for 30 min. The entire preparation was performed on ice to limit warm ischemia and proteolysis.

Intestinal enterocytes were isolated by calcium elution. Solution B (pH 7.4) contained Dulbeccos phosphate buffered saline, 5 mM EDTA, 0.5 mM DTT and protease inhibitor cocktail with 9 UI/ml heparin. Intestines were flushed with solution B, the elutant collected and then filled until distended with solution B, sealed, and agitated vigorously for 15 min in a sealed container with incubation buffer solution (pH 7.2) consisting of Dulbeccos phosphate buffered saline and 20% v/v glycerol. Solution B was collected and intestines flushed with solution B, refilled, sealed and re-agitated for a further 15 min. The collected eluent was centrifuged at 2 000 g for 10 min at 4°C. The pellet was taken up by 3–4 ml per g of cells of solution C. (pH 7.4) which contained Dulbeccos phosphate buffered saline, 0.25 M sucrose, 0.5 mM EDTA, 5 mM histidine and protease inhibitor cocktail. Disruption of cells was achieved using a Potter-Elvejhem rotating homogenizer and an ultrasonic probe (Branson Ultrasonics, Danbury, CT, USA). A sample of homogenate was then collected for protein and correction-for-loss experiments. Homogenate was ultracentrifuged at 10 000 g (Optima LE-80 K, Beckman Coulter, 50.2Ti rotor) for 15 min 4°C. The resulting 'S9' supernatant was filtered through NYTAL filter mesh (pore size: 150 μm) (Lockertex, Warrington, UK) and then ultracentrifuged for 70 min at 100 000 g at 4°C. The final pellet was re-suspended in Tris–HCl buffer (pH 7.4) containing protease inhibitor cocktail. Protein concentrations of microsomal and homogenate samples were determined using the Bicinchoninic acid assay (Pierce Biotechnology, IL, USA). Remaining yields were stored at−80°C prior to transfer to the laboratory for further analysis.

Measurement of Enzyme Activity

7-ethoxyresorufin de-ethylation (EROD), a reaction mediated by canine CYP1A1, CYP1A2 and CYP2A13 [27–29], was measured in liver homogenates and microsomes and was used as a marker of recovery of CYP activity during preparation of microsomes. Similarly, midazolam-1'-hydroxylation (a marker of CYP2B11 activity [30]) was used as the functional marker for CYP recovery in intestinal microsomes. Additionally, 7-hydroxy-4-trifluoromethylcoumarin (HFC) glucuronidation, a reaction attributed to several UGT enzymes [31] was measured both in liver and intestinal homogenates and microsomes.

For EROD measurements, 100 μL of liver homogenates and microsomes in 100 mM Tris–HCl buffer, pH 7.4, containing 7-ethoxyresorufin was pre-incubated at 37°C for 10 min. The reactions were initiated by adding 50 μl of pre-heated NADPH-regenerating system (consisting of 1.13 mM NADP, 12.5 mM isocitric acid, 56.33 mM KCl, 12.5 mM $MgCl_2$, 0.0125 mM $MnCl_2$ and 0.075 U/mL isocitrate dehydrogenase in 187.5 mM Tris–HCl at pH 7.4). Final 7-ethoxyresorufin and protein concentrations in incubations were 4 μM and 0.2 mg/mL, respectively. After 30 min incubation the reactions were terminated by addition of 110 μl stop solution (consisting of 80% acetonitrile and 20% 0.5 M Tris) and formation of resorufin was quantitated by measuring fluorescence (570 nm excitation and 615 nm emission) with Victor^2 ™ 1,420 Multilabel Plate Reader (PerkinElmer/Wallac).

Midazolam 1'-hydroxylation was measured by incubating 15 μM midazolam in the presence of intestinal homogenates

and microsomes (0.5 mg/ml protein in 300 µl volume) in 100 mM Tris–HCl buffer (pH 7.4) and 1 mM NADPH at 37°C. 100 µl samples were withdrawn at 30 min and mixed immediately with 100 µl ice-cold acetonitrile to stop the reaction. The amount of 1'-hydroxymidazolam formed was quantitated using HPLC-MS.

HFC glucuronidation in dog liver homogenates and microsomes (DLH and DLM, respectively) and dog intestinal homogenates and microsomes (DIH and DIM, respectively) was measured as described earlier [31]. Briefly, 20 µM HFC was incubated with 0.2 mg/mL (DLM and DLH) or 0.5 mg/mL (DIM and DIH) in the presence of 1 mM UDPGA at 37°C and the decay of HFC was followed by measuring fluorescence (364 nm excitation and 498 nm emission) once per minute for 20 min using an EnVision® 2,104 Multilabel reader (PerkinElmer/Wallac) multi-well reader. HFC clearance was calculated from the slope of the log HFC concentration *versus* time curve.

Mass Spectrometry Quantitation of CYP and UGT Enzymes

Denaturation and Digestion of Tissue Homogenate and Microsome Samples

In addition to intestine and liver tissue homogenate and microsome samples collected from the Roche Nutley dog colony, four liver and four intestinal (segment SI4) microsome samples from Celsis In Vitro Techologies used in our previous study [24] were used for assay development for UGT enzyme quantitation and were included in the current proteomic analysis.

Homogenate and microsome samples (25 µl suspensions containing known amount of total protein, approximately 500 µg) were denatured by addition of trifluoroethanol and ammonium bicarbonate to final concentrations of 50% (v/v) and 125 mM respectively. Cysteines were reduced by addition of 16 mM 1,4-dithioerythritol followed by incubation at 65°C for 1 h. Samples were then cooled and cysteines blocked by addition of 40 mM iodoacetamide followed by incubation at 20°C for 30 min in the dark. Excess iodoacetamide was blocked by addition of 7 mM 1,4-dithioerythritol followed by vortexing. Samples were then diluted with 0.1 mM Tris–HCl, pH 8.0 to reduce the trifluoroethanol concentration to 5%. Trypsin (Roche, sequencing grade) was then added (1:20 trypsin:total protein w:w) followed by incubation at 37°C overnight (16 to 18 h). Digestion was stopped by addition of 1% formic acid. Prior to mass spectrometry analysis, digested samples were diluted with LC buffer A (water, 2% acetonitrile and 0.1% formic acid) containing stable isotope-labelled internal standards to give a final sample protein concentration of 100 ng/µl and internal standard concentration of 2 fmol/µl. Thus, internal standard concentration corresponded to 20 pmol/mg of total protein.

Selection of Synthetic Peptides for CYP Quantitation

The heavy labeled peptide standards used for CYP quantitation in an earlier study [24] (AQUA Ultimate grade from Thermo Fisher Scientific GmbH, Ulm, Germany) were also used in the current work (Table 1). Two of the three CYP1A2 peptides were not used for quantitation of CYP1A2 since they are affected by SNPs in the gene encoding this protein [32] and thus were not present in some of the donors. Also, the data on the long hydrophobic peptide for CYP2B11 (NLIDTALSLFFAGTETTSTTLR) suggested compromised stability of the heavy labeled standard during the storage and consequently the data on this peptide were not used for final assessment of protein abundance. Although two of the three peptides used for quantitation of CYP2D15 have been reported to be mutated in the allele variant CYP2D15 V1 [33], these peptides were present in all liver samples suggesting that the variant CYP2D15 V1 was not carried by any of the donors. Consequently, these peptides were retained for quantitation of CYP2D15.

Selection of Synthetic Peptides for UGT Quantification

Amino acid sequences and nomenclature of beagle dog UGT enzymes was adapted from [34–36].

Samples, corresponding to one microgram of total protein, from four liver and four intestinal microsome batches were analyzed on an LTQ Orbitrap XL (Thermo Fisher Scientific). Tryptic peptides were separated by reverse-phase chromatography with a Proxeon EASY-nLC II liquid chromatography system (Thermo Fisher Scientific) connected to an RP-HPLC column (75 µm × 10 cm) packed with Magic C18 AQ (3-µm) resin (WICOM International). Peptides were eluted with 0.1% formic acid and 98% acetonitrile (solvent B) as the mobile phase, following a linear gradient from 5% to 35% over the stationary phase (solvent A: 0.1% formic acid and 98% acetonitrile) at a flow rate of 300 nl/min. The data-acquisition mode was set to obtain one high-resolution mass spectrometry scan in the Orbitrap (60,000 at 400 m/z) and to select the ten most abundant ions for collision-induced fragmentation, with omission of unassigned or single-charge states. The dynamic exclusion window was set to 30 s and was limited to 300 entries. Only mass spectrometry precursors that exceeded a threshold of 150 ion counts were allowed to trigger tandem mass spectrometry scans. The ion-accumulation time was set to 500 ms (mass spectrometry) or 250 ms (tandem mass spectrometry) with a target setting of 106 ions (mass spectrometry) or 104 ions (tandem mass spectrometry). The resulting tandem mass spectrometry fragment ion spectra were acquired in the linear trap quadrupole. The

Table I The peptides used in SRM assay for beagle dog CYP enzymes

Protein	Peptide sequence	Used for protein quantitation	Comment
CYP1A2	EAEALLSR	–[a]	Polymorphic, peptide not present in all donors
	SVQDITGALLK	+[a]	
	FLTADGTTINK	–	Polymorphic, peptide not present in all donors
CYP2B11	GIIQPEKPVVLK	+	
	EALVDNAEAFSGR	+	
	QVYNNLQEIK	+	
	NLIDTALSLFFAGTETTST TLR	–	Heavy peptide standard compromised during storage
CYP2C21	FSLTVLR	+	
	DFIDYFLIK	+	
	YGLLVLLK	+	
CYP2D15	VQQEIDEVIGR	+	Mutated in allele variant CYP2D15 V1 (33), peptide present in all liver donors
	GTTLITNLSSVLK	+	
	DTEVQGFLIPK	+	Mutated in allele variant CYP2D15 V1 (33), peptide present in all liver donors
CYP2E1	GEVFAFQSHK	+	
	GITFNNGPGWK	+	
	EIPFLLEALR	+	
CYP3A12	LQEEIDATFPNK	–	Shared peptide, CYP3A12/26
	DVEISGVFIPK	–	Shared peptide, CYP3A12/26
	LNAQGIIQPEKPIVLK	+	
CYP3A26	LQEEIDATFPNK	–	Shared peptide, CYP3A12/26
	DVEISGVFIPK	–	Shared peptide, CYP3A12/26
	GIIQPEKPVVLK	+	

[a] – and + indicate that the quantitation data on the peptide was not and was used for estimation of protein quantity, respectively

acquired MS2 spectra were searched against a dog protein database (compiled at Roche based on publicly available dog proteome and genome data) using Sequest as search engine on the Trans-Proteomic Pipeline. The search parameters were set to include only fully tryptic peptides (KR/P) containing up to two missed cleavage sites. Carbamidomethyl (+ 57.021465 Da) on cysteine was set as static peptide modification. Oxidation (+15.99492 Da) of methionine was set as dynamic peptide modifications. The precursor mass tolerance was set to 25 p.p.m., and the fragment mass error tolerance was set to 0.5 Da. The peptide spectrum matches obtained were evaluated statistically with the PeptideProphet program for confirming peptide assignments to tandem mass spectrometry spectra and protein inference was evaluated by the ProteinProphet program for confirming protein identifications made on the basis of peptides assigned to tandem mass spectrometry spectra (both part of the Trans-Proteomic Pipeline collection of integrated tools, version 4.5.1). A minimum protein probability of 0.9 was set to match a false-discovery rate of <1%. Only peptides at false discovery rate of <1% were considered for further analysis. The PeptideProphet output from above was processed with Skyline software [37] to generate a spectral library. The occurrence of fragment ion interferences and number of unique transitions per peptide were computed using the tool "SRM collider" against a dog background without missed cleavages [38]. For each protein, two proteotypic peptides were selected when possible. Only fully tryptic peptides without missed cleavages and a length between 6 and 21 amino acids were allowed. Furthermore, highest priority was given to peptides with the highest number of previous detection by shotgun. Stable isotope-labeled peptides with C-terminal 15 N- and 13C-labeled arginine or lysine residue (>99 atom % isotopic enrichment, AQUA QuantPro grade), corresponding to 13 UGT proteins (Table 2), were purchased from Thermo Fisher Scientific GmbH (Ulm, Germany).

Development and Validation of SRM Assays for UGT Enzymes

The synthetic peptides were mixed and spiked into the digested liver and intestinal microsome samples and measured on the TSQ vantage Triple Quadrupole Mass Spectrometers (ThermoFisher, San Jose, CA). If available, the six highest fragment ion peaks belonging to the y-ion series of the 2+ and 3+ precursors were extracted from the spectral library using Skyline [37]. The transition groups were measured in non-scheduled and scheduled SRM acquisition mode. A spray voltage of 1.3 keV was used with a heated ion transfer tube set at a temperature of 280°C. Chromatographic separations of peptides were performed on a NanoLC-2Dplus HPLC system (Eksigent, Dublin, CA) coupled to a 10 cm fused silica emitter, 75 μm diameter, packed with a Magic C18 AQ 5 μm resin (Michrom BioResources, Auburn, CA, USA). Peptides were loaded on the column from a cooled (4°C) Eksigent autosampler and separated with a linear gradient of acetonitrile/water, containing 0.1% formic acid, at a flow rate of 300 nL/min. A gradient from 5 to 35% acetonitrile in 40 min was used. The mass spectrometer was operated with selected reaction monitoring (SRM). Acquisitions Q1 and Q3 were obtained at 0.7 unit mass resolution. Transitions were

Table 2 The peptides used for quantitation of beagle dog UGT enzymes in SRM experiments

Protein	Peptide sequence	Used for protein quantitation	Comment
UGT1A1	GVFENVPLLR	+[a]	
	EDVEATFTSLGR	+	
UGT1A2	TATLIFQR	+	
	EVSLEDILSSGSVWLFR	–	High unexplained variability, peptide not used for quantification
UGT1A3	ILLGQSYLVFER	+	
	AAALIFQR	+	
UGT1A4	EEDFFTLTTYAPPYTR	+	
	TVTSFYQR	+	
UGT1A6	YEDLASNILK	+	
UGT1A7	ADFVLDYPK	+	
UGT1A8	–	–	Proteotypic peptides not identified
UGT1A9	DTTLIEYIK	+	
	TFSDSHWNIR	+	
UGT1A10	NFSDSHWNIR	–	Predicted peptide, reliable detection not achieved
UGT1A11	TFSDSQWNIR	+	
	TYSTTYNLEELNQK	+	
UGT2A1	IIIDELIK	–	Predicted peptides, reliable detection not achieved
	NILLLSLK	–	
UGT2A2	IILEELIQR	–	Predicted peptides, reliable detection not achieved
	LLDTFFR	–	
	INIQICDGVLSNPK	–	
UGT2B31	ANVIASALAQ	+	
	IPQKIPLVYSLR	+	

[a] – and + indicate that the quantitation data on the peptide was not and was used for estimation of protein quantity, respectively

recorded for the endogenous (light) and the internal standard (heavy) peptides. For the scheduled acquisition mode time-based SRM was used to achieve a high dwell time (*i.e.* > 50 ms) for each transition, where an acquisition time window of 3 min was set around their elution time. Full-scans were monitored during 1 s and between m/z values of 350 and 1 350. Argon was used as the collision gas at a nominal pressure of 1.5 mTorr. Collision energies for each transition were calculated according to the "in house" developed equations: CE = 0.034 * (m/z) -0.848 and 3+: CE = 0.022 * (m/z) + 5.953 (CE, collision energy and m/z, mass to charge ratio) for doubly and triply charged precursor ions, respectively. SRM data were processed using Skyline software. The three most abundant transitions for each 12C/13C pair were selected and used to quantify the peptide unless signals of co-eluting interferences were also detected. In such cases, only transitions having no distinct contamination in the SRM channel were used.

SRM Quantitation of CYP and UGT Proteins

Peptide quantitation by selected reaction monitoring (SRM) was performed using an Ultimate 3 000 n-liquid chromatography (LC) system (ThermoFisher Scientific) coupled to a TSQ Vantage extended mass range triple quadrupole mass spectrometer (ThermoFisher Scientific, San Jose, CA, USA). Samples (5 µl, 500 ng total protein, 10 fmol internal standard) were loaded onto a trap column (ACE C18 3 µm 300 Å, 5 mm × 300 µm) at 50 µl/min in buffer A (water, 2% acetonitrile and 0.1% formic acid) for 2 min. Following sample loading, peptides were resolved on an analytical column (ACE C18 3 µm 300 Å, 10 cm × 75 µm, ACT) at 500 nl/min. The column was heated to 30°C. The following gradient was used: 0 min, 98% A, 2% B (acetonitrile, 0.1% formic acid); 2 min, 2% B; 3 min, 8% B; 17 min, 30% B; 18 min, 80% B; 21 min, 80% B; 22 min, 2% B; 30 min 2% B. The LC eluent was interfaced with the TSQ Vantage with a picotip emitter (20 µm i.d., 10 µm tip i.d., New Objective). The TSQ Vantage was operated in SRM mode and measured 120 transitions in parallel for the CYP method and 138 transitions for the UGT method. In both cases scheduled SRM was used to ensure the maximum number of concurrent transitions was below 80 for the CYP method and 100 for the UGT method respectively. A scan time of 1.5 s was used and a collision gas setting of 1.5 mTorr argon for the CYP method and 1.2 mTorr argon for the UGT method respectively. The selectivity for both Q1 and Q3 was set to 0.7 m/z unit (FWHM). The SRM transitions and collision energies are listed in the data supplement (Table 2-S).

Raw SRM data was processed using Skyline v1.4 [37]. Peak integrations were reviewed manually and transitions from endogenous peptides were confirmed by comparing retention times and relative transition intensities with those of the synthetic heavy stable isotope-labeled peptides. The amount on the column for individual transitions was calculated based on heavy to light peak area ratio and the data were exported to an Excel file for statistical analysis.

Data Analysis

A linear mixed effects (LME) modeling approach was employed to summarize the SRM quantitation data using

JMP® Pro (version 11.0.0, SAS Institute Inc.) software. To obtain CYP and UGT protein abundances in individual samples a LME model (Eq. 1) [24] was fitted to log transformed SRM quantitation data.

$$M = Sample + Peptide(R) + Transition[Peptide](R) \quad (1.)$$

Where M is the log transformed SRM quantitation result for an individual transition, the estimates for the fixed effect Sample are taken as the protein abundance in the sample. Peptide effect and Transition effect nested within Peptide are considered as random effects denoted by (R) in the equation.

To estimate biological variability in the CYP and UGT abundance measurements in liver samples and to establish estimates of inter-individual variability, a LME model including a fixed effect for the sample type (homogenate or microsome) and a random effect for the donorID was fitted to log transformed to log transformed SRM quantitation data.

$$M = SampleType + Donor(R) + Peptide(R) + Transition[Peptide](R) \quad (2.)$$

The estimates for the fixed effect SampleType were taken as the typical enzyme abundance in DLM and DLH. As LME modeling was done and the resulting variance estimates are on log transformed data, coefficient of variation (CV) describing biological variability was calculated according to Eq. 3 from the variance (σ^2) component of log transformed data attributed to Donor effect. Residual variability, *i.e.* that part of variance not explained by the effects of transition, peptide, sample type (homogenate or microsome) or biological variability was taken as the technical variability. Biological variability in hepatic enzyme abundance was estimated separately within the Roche Nutley dog colony ($N = 14$) and within the whole set of donors ($N = 18$).

$$CV = \sqrt{exp^{\sigma^2} - 1} \quad (3.)$$

Abundance of CYP and UGT proteins and three enzyme activity markers, EROD (only in liver samples), midazolam 1'-hydroxylation (only in intestinal samples) and HCF glucuronidation (both liver and intestine) were measured both in homogenates and corresponding microsomes. This allowed calculation of microsomal enrichment of these individual markers, which enables accounting for inability of the cell fractionation protocol to completely recover microsomal protein, according to Eq. 4

$$Fold\ enriched = {}^{marker_{mic}} / marker_{hom} \quad (4.)$$

$marker_{mic}$ and $marker_{hom}$ refer to CYP or UGT abundance or activity per milligram of protein in microsomes and homogenates, respectively. In addition to individual markers the fold enrichment was also calculated using the sum of CYP proteins and sum of UGT proteins as microsomal markers.

The fold enrichment, together with the yields of homogenate protein (HP_{yield}) and microsomal protein (MP_{yield}) allowed calculation of fraction of microsomal protein recovered (Eq. 5) and, consequently, accounting for losses during cell fractionation when estimating of the total amount of microsomal protein (MP) in intact tissue (Eq. 6).

$$Fraction\ recovered = \frac{MP_{yield}}{HP_{yield}} * Fold\ enriched \quad (5.)$$

$$MP = {}^{HP_{yield}} / Fold\ enriched \quad (6.)$$

The fold enrichment and fraction recovered for each marker were calculated separately for each batch of microsomes and the results were summarized by fitting a LME model (Eq. 7) to log transformed results.

$$F = Marker + Batch(R) \quad (7.)$$

F is the fold enriched (or fraction recovered) calculated for an individual marker in an individual tissue processing batch and the fixed effect Marker is taken as an estimate of typical fold enrichment (or fraction recovered) for the given marker.

Estimates of the amount of microsomal protein (MP) in intact tissue were calculated using the fold enrichment of the sum of CYPs and the sum of UGTs.

Statistical significance of differences in the levels of the fixed effects was tested by computing Tukey's HSD test.

RESULTS

Abundance and Activity of CYP and UGT Enzymes in Dog Gut Wall and Liver

Abundances of CYP and UGT proteins in intestinal and liver homogenates and microsomes are summarized in Fig. 1 and

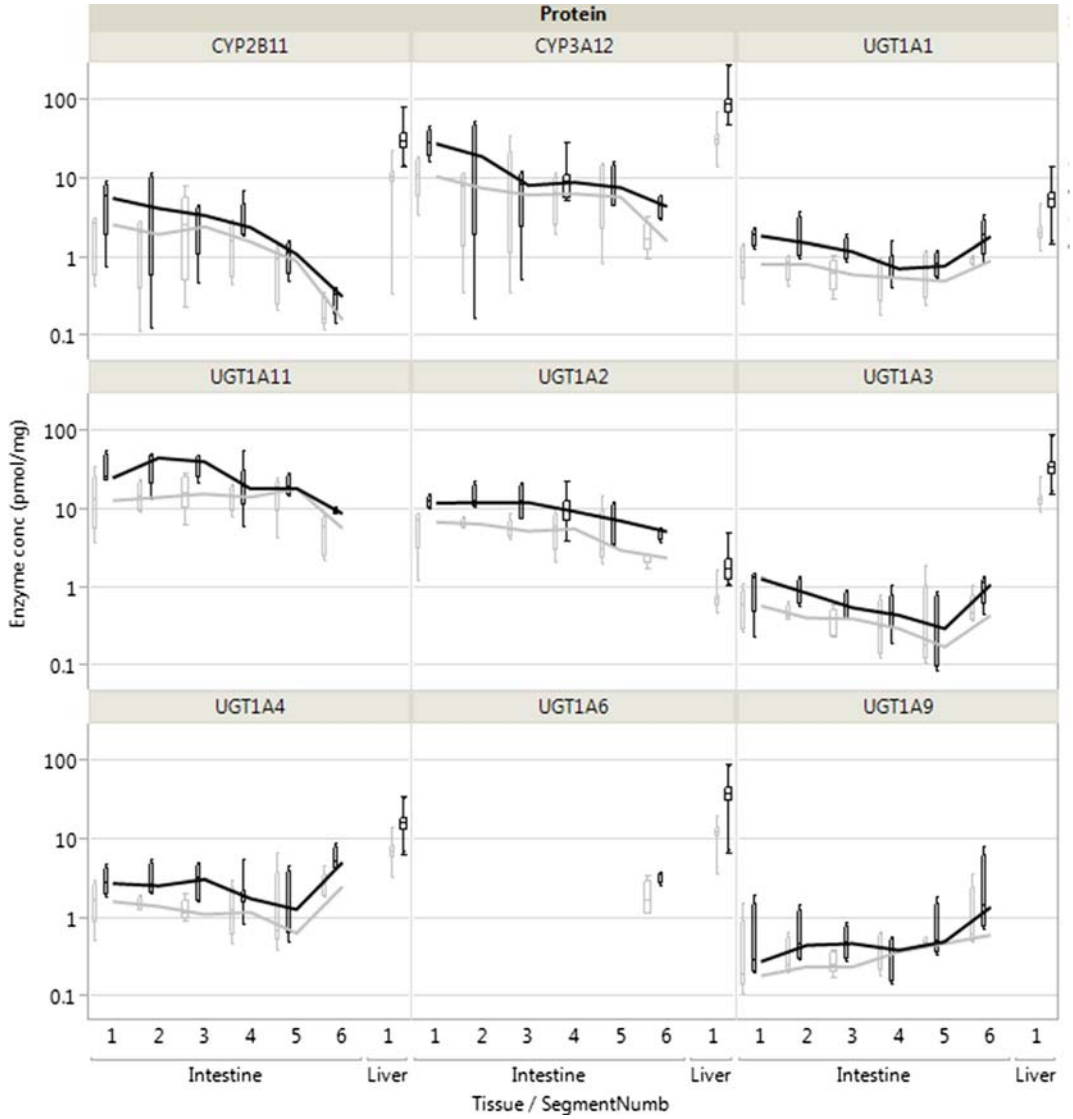

Fig. 1 CYP and UGT enzyme abundance in the beagle dog enterocyte homogenates (*grey*) and microsomes (*black*). Abundance in the liver is shown for comparison. The boxes represent the interquartile range, the horizontal line is the median and the whiskers show the lowest and highest values. Data are from 5 donors, except microsomes of segment 4 are from 9 donors. Solid lines are drawn through the medians to visualize the profile along the intestine. Segment numbering starts from the proximal intestine and numbers 1–5 and 6 refer to small intestine and colon, respectively. UGT1A6 was not quantifiable in the small intestine samples and UGTs 1A9 and 1A11 were not quantifiable in the liver

Table 3. Both CYPs and UGTs are microsomal proteins and were enriched approximately 1.5 to 3.5 fold in microsomal fractions compared to corresponding homogenate samples (Tables 5 and 6). Measurement of microsomal enrichment enabled evaluation of losses during cell fractionation and estimation of the total amount of microsomal protein in intact tissues (below).

7 CYPs and 7 UGTs were quantifiable in the liver. CYP3A12 was the most abundant CYP at approximately 30% of the total CYP amount, whereas UGT2B31 was the most abundant UGT constituting approximately 70% of total UGT enzyme amount (data supplement, Figure 1-S). In the liver samples the total amount of CYP enzyme quantitated was similar to the total amount of UGT enzyme. In contrast, the total amount of UGTs in intestinal samples was up to 4 times higher than the total amount of CYPs with a trend towards a larger difference in distal intestine (data supplement, Figure 2-S).

2 CYPs and 8 UGTs were quantifiable in the intestinal samples (Fig. 1). As reported earlier [9], CYP3A12 and CYP2B11 were present in both intestine and liver and showed a declining trend from proximal to distal intestine. They were both at higher concentration (as pmol/mg of microsome or homogenate protein) in the liver than in the intestine. CYP3A12 and CYP2B11 constituted approximately 90% and 10%, respectively, of total CYP quantitated in the proximal and distal intestine whereas in the segments 2, 3 and 4 of small intestine corresponding percentages were

Table 3 Estimates of Typical CYP and UGT Abundance, Biological Variability and Technical Variability in Beagle Dog Liver Homogenates (DLH) and Microsomes (DLM) when Using Data from Both Roche Nutley ($n=14$) and Covance ($n=4$) Dog colonies

Enzyme	Typical abundance (pmol/mg prot)		Biological CV%[a]	Technical variability CV% [a]
	DLH	DLM		
CYP1A2	13	37	60 (31–82)	21 (20–22)
CYP2B11	12	35	34 (19–44)	23 (22–23)
CYP2C21	21	70	23 (13–31)	22 (21–23)
CYP2D15	19	56	39 (22–52)	22 (22–23)
CYP2E1	13	36	41 (23–55)	25 (24–25)
CYP3A12	32	93	33 (18–44)	21 (20–23)
CYP3A26	1.1	2.7	34 (18–46)	38 (36–41)
UGT1A1	2.5	6.0	50 (28–68)	20 (20–21)
UGT1A2	0.87	2.0	46 (25–62)	23 (22–24)
UGT1A3	14	35	29 (16–39)	26 (25–27)
UGT1A4	7.6	17	32 (17–42)	29 (28–30)
UGT1A6	12	36	54 (29–74)	27 (26–29)
UGT1A7	2.3	5.8	74 (39–105)	25 (24–27)
UGT2B31	108	274	40 (22–53)	19 (19–20)

[a] Biological and technical CV% were calculated from the variance components attributed to biological differences and residual variability, respectively, using Eq. 3. The values in parenthesis show the 95% confidence interval for the estimated CV%

approximately 70% and 30% for CYP3A12 and CYP2B11, respectively (data supplement, Figure 3-S).

UGTs 1A1, 1A3, 1A4 and 1A6 were more highly abundant in the liver than in the intestine (as pmol enzyme per mg of microsome or homogenate protein) and 1A7 and 2B31 were present in the liver but not detected in the intestine (Fig. 1, Table 3). UGT1A11, the most abundant enzyme in the intestinal samples, and UGT1A9 were not detectable in the liver. In addition, UGT1A2, also highly abundant in the intestine, was present only at low amounts in the liver samples. Furthermore, in contrast to the decreasing trend of CYP abundance towards the colon, the abundances of many UGT enzymes were at similar (UGTs 1A1 and 1A3) or higher (UGTs 1A4, 1A6 and 1A9) levels (as pmol/mg of microsome or homogenate protein) in the colon than in the small intestine. The relative contribution of individual UGT enzymes to the total amount of UGTs measured in intestinal samples remained fairly constant throughout the small intestine with UGT1A11 and UGT1A2 constituting approximately 60% and 25%, respectively. In the colon UGT1A11, UGT1A2, UGT1A4 and UGT1A6 constituted approximately 35%, 20%, 20% and 10% of total UGTs respectively (data supplement, Figure 4-S).

Proteotypic peptides predicted for UGTs 1A10, 2A1 and 2A2 were not quantifiable in either of the tissues and this study could not provide information on the abundance of UGT1A8 as proteotypic peptides were not identified (Table 2).

Preparation of liver tissue samples in triplicate allowed for separation of biological and technical variability in CYP and UGT abundance. The CV estimates for biological variability of CYP and UGT enzymes ranged from 33 to 60% and from 29 to 74%, respectively, when data from all donors ($n=18$) were used for analysis (Table 3) and were systematically smaller when only the data from donors from the Roche Nutley dog colony ($n=14$) were used (Table 4). As only the samples from the Roche Nutley dog colony included technical replicates of tissue processing, the analysis assumed that technical variability is similar for samples from both sources and varied from 20 to 40% depending on the enzyme.

HFC glucuronidation clearance (pmol/min/mg protein) was approximately 6 fold higher in the liver samples than in the intestinal samples and a clear correlation with any individual UGT enzyme abundance was not found (data not shown). There were substantial differences in midazolam 1'-hydroxylation rate between intestinal segments with some of the segments being below the limit of quantitation of the assay (0.1 pmol/mg/min). The segments with low CYP2B11 and CYP3A12 abundance showed low midazolam 1'-hydroxylation rate whereas high CYP2B11 and CYP3A12 abundance was not always reflected as a high rate. However, the segments with a low midazolam 1'-

Table 4 Estimates of Typical CYP and UGT Abundance, Biological Variability and Technical Variability in Beagle Dog Liver Homogenates (DLH) and Microsomes (DLM) When Using Data Only from the Roche Nutley Dog Colony ($n=14$)

Enzyme	Typical abundance (pmol/mg prot)		Biological CV%[a]	Technical variability CV%[a]
	DLH	DLM		
CYP1A2	11	32	37 (17–51)	21 (20–22)
CYP2B11	11	30	16 (8–22)	23 (22–24)
CYP2C21	21	70	18 (9–24)	22 (21–23)
CYP2D15	19	54	29 (14–40)	21 (21–22)
CYP2E1	11	31	30 (14–40)	25 (24–26)
CYP3A12	31	91	21 (10–28)	22 (21–23)
CYP3A26	1.2	2.9	26 (12–36)	39 (37–41)
UGT1A1	2.1	4.8	28 (13–38)	21 (20–22)
UGT1A2	0.7	1.6	20 (9–26)	23 (22–25)
UGT1A3	13	32	15 (7–20)	26 (25–27)
UGT1A4	6.8	15	21 (10–29)	29 (28–30)
UGT1A6	12	36	14 (6–19)	28 (27–30)
UGT1A7	2.2	5.4	49 (22–68)	25 (24–27)
UGT2B31	90	228	15 (7–20)	20 (19–21)

[a] Biological and technical CV% were calculated from the variance components attributed to biological differences and residual variability, respectively, using Eq. 3. The values in parenthesis show the 95% confidence interval for the estimated CV%

hydroxylation rate showed this consistently in both homogenate and corresponding microsome samples (Fig. 2).

One donor (out of 18) did not carry any CYP1A2 peptides. This is consistent with SNP 1,117 C>T which is homozygously carried by ~10% of beagle dogs [39] and results in a stop codon with consequent deletion of the protein. This donor was not accounted for when estimating the typical value and inter-individual variability for CYP1A2 abundance in the beagle dog liver. Two other SNPs in the dog CYP1A2 gene which result in changes in the peptides measured in this study have been reported in the literature [32] (Table 1). SNP 500 C>T, resulting in replacement of alanine with valine in position 167, was probably carried by 1 donor as the wild type peptide EAEALLSR was not present in this donor while the peptide not affected by known polymorphisms, SVQDITGALLK, was present. SNP 1,303 A>G, resulting in replacement of alanine with threonine in position 435, was detected in 3 donors (the mutated form peptide, FLATDGTTINK was present). However, there was no evidence of altered CYP1A2 abundance or activity in these donors (Fig. 3).

For the intestine, 9 proteins and 2 activity markers were used (Table 5 and Table 6). Microsomal enrichment in intestine was approximately 10–15% and tended to be lower than in liver (35–50%). There was no observable difference in enrichment between intestinal segments (data not shown). In general, enrichment of the enzyme activity markers did not stand out as different from the recovery of the protein abundance markers. However, there were small but statistically significant differences between microsomal enrichment of individual markers in the liver (Table 5). Correspondingly, the trends in microsomal enrichment of different markers are reflected as similar trends in the microsomal recovery of the markers.

Estimates of the amount of total microsomal protein in the dog liver and intestine calculated based on the recovery of sum of CYPs and sum of UGTs are presented in Table 7 and Figure 5–S (data supplement). Meaningful estimates of the biological variability in the total microsomal protein abundance were not obtained in either of the tissues because the 95% confidence interval of the variance attributed to between donor differences included 0.

Microsomal Enrichment of CYP and UGT Enzymes and Estimated Amount of Total Microsomal Protein in Tissue

Microsomal enrichment for liver samples was calculated based on the abundances of 14 proteins and on 2 activity markers.

DISCUSSION

Beagle dog is used as an animal model to study oral pharmacokinetics, food effects and formulation behavior during

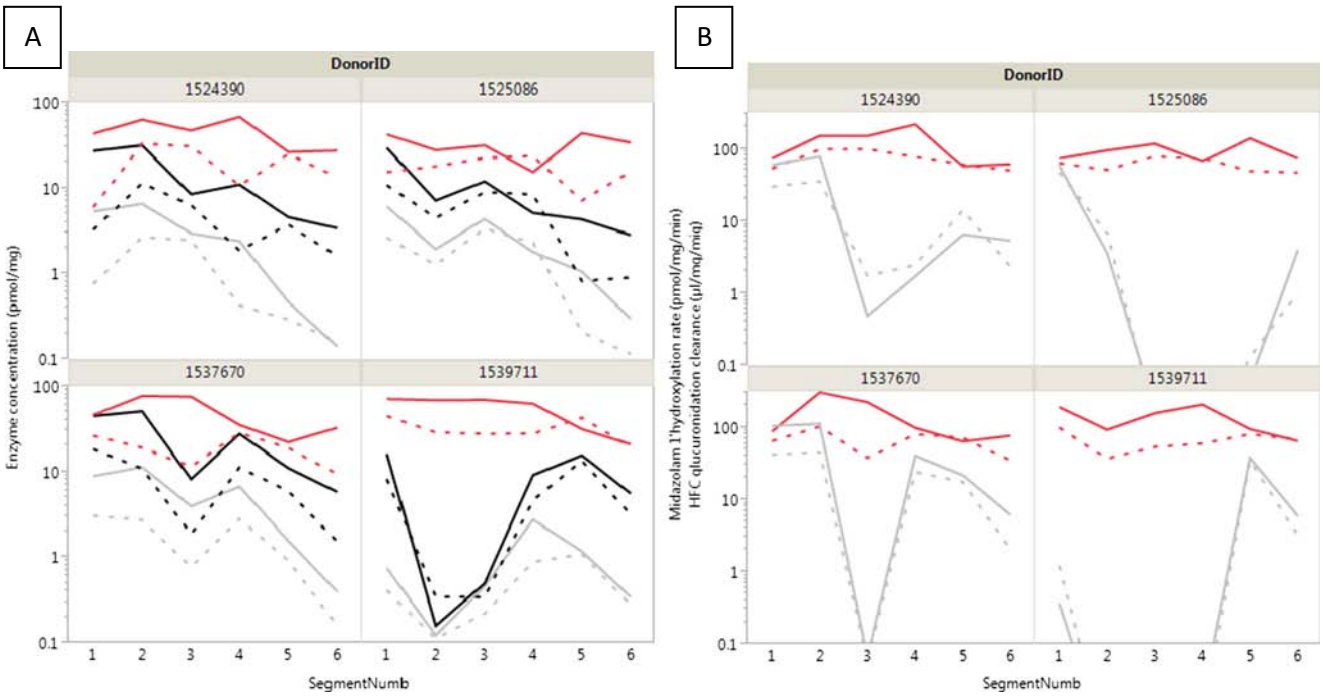

Fig. 2 CYP and UGT enzyme abundance and activity in beagle dog intestine. Segment numbering starts from the proximal intestine and numbers 1–5 and 6 refer to small intestine and colon, respectively. (**a**) CYP2B11 (*gray*), CYP3A12 (*black*) and Sum-of-UGTs (*red*) abundance in beagle dog intestinal microsomes (solid line) and homogenates (*dashed line*). (**b**) Midazolam 1'-hydroxylation rate (gray) and 7-hydroxy-4-trifluoromethylcoumarin glucuronidation clearance (*red*). The low limit of quantitation of midazolam 1'-hydroxylation was 0.1 pmol/mg/min

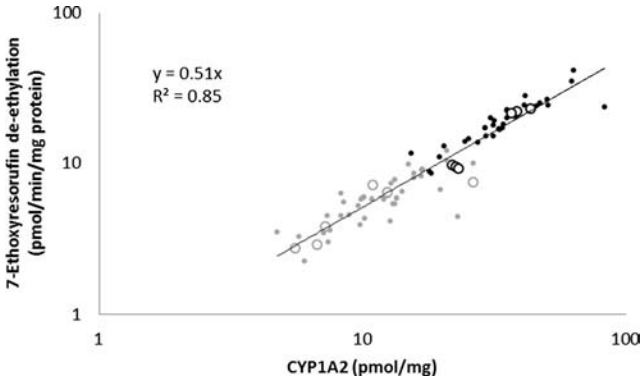

Fig. 3 7-ethoxyresorufin de-ethylation (EROD) rate *versus* CYP1A2 concentration in dog liver microsomes (*black*) and homogenates (*grey*). 4 μM 7-ethoxyresorufin was incubated in presence of 0.2 mg/mL liver homogenate or microsome protein. Each symbol represents the mean of two EROD measurements and the linear regression line was fitted through the origin using all the shown data points. The results show a clear correlation between EROD activity and CYP1A2 abundance and suggest no difference in this correlation between donors who carry mutation 1,303 G > A (donors carrying peptide 428_FLATDGTTINK, open symbols. Twelve samples in total, three batches of liver homogenates and microsomes from two donors) and donors who do not carry this mutation (closed symbols)

development of drugs intended for human use. However, there are many gaps in our understanding of factors determining PK and its' variability in the dog and research on the abundance and activity of metabolic enzymes has recently been advocated by the FDA from both human drug development and veterinary medicine perspectives [26]. This paper has described quantification of the abundances of 7 CYP enzymes and 9 UGT enzymes in enterocyte and liver homogenates and microsomes from beagle dogs using SRM mass spectrometry. Additionally, inability to detect the predicted proteotypic peptides for 3 additional UGT enzymes (UGT1A10, UGT2A1 and UGT2A2) suggests absence or negligible abundance of these proteins in these tissues. In addition, this work has provided estimates of biological variability in hepatic enzyme abundance providing a basis for bottom up prediction of variability using PBPK modeling.

CYP and UGT abundance and activity in dog liver and intestine

The results of this study on CYP abundance are in agreement with the results of the smaller study we reported earlier [24]. Furthermore, the results of these studies using SRM quantitation of beagle CYP proteins are in general accordance with immunologically based quantitation results reported in the literature [26, 40–43].

Current and previous SRM [24] studies on dog CYP protein abundance suggest that CYP3A12 is the most abundant CYP enzyme in both liver and intestine whereas the contribution of CYP3A26 is minimal in both tissues. This is partially in accordance with literature reports on CYP3A12 and CYP3A26 mRNA expression. Total CYP3A gene expression was reported to be greater in the liver than in the intestine and intestinal CYP3A12 expression was greater than that of CYP3A26 [44]. However, CYP3A26 was reported to comprise the majority of the hepatic CYP3A mRNA pool [44, 45]. Due to the high similarity of CYP3A12 and CYP3A26, only one proteotypic peptide was measurable for each of these enzymes in the current study. Thus, it is possible that the low apparent CYP3A26 abundance in the liver is due to bias in quantitation of the single CYP3A26 proteotypic peptide. Arguing against this possibility is that preliminary experiments with recombinant enzymes (data not shown) suggested similar performance for the proteotypic peptides used for CYP3A12 and CYP3A26. Furthermore, the quantitation results on the two peptides that are shared for these two proteins (Table 1) are similar to results of the proteotypic peptide for CYP3A12 (supplementary Excel data sheet), further supporting the conclusion that the reported high CYP3A26 gene expression in the dog liver is not reflected in high protein abundance.

Midazolam 1'-hydroxylation was measured in dog intestinal homogenates and microsomes. This reaction is primarily mediated by CYP2B11, with only a minor contribution from CYP3A12 [30] and the lack of correlation between CYP2B11 abundance and midazolam 1'-hydroxylation activity (Fig. 2) suggests that activity was lost during tissue processing. Furthermore, the consistency of activity measurements in homogenate and corresponding microsome samples suggests that the loss occurred prior to preparation of enterocyte homogenates rather than during cell fractionation or sample storage. The reason(s) for loss of function in some, but not all, of the intestinal segments can only be speculated as current data do not allow us to trace this back to differences in handling. It is interesting to observe that similar loss of metabolic activity is not reflected in the HFC glucuronidation, suggesting that CYP2B11 may be more vulnerable to loss of activity than the UGT enzymes. Similarly, our previous study on dog CYPs [9] suggested that specific activity of CYP2B11 and CYP3A12 (measured as diazepam demethylation and 3-hydroxylation, respectively) is substantially smaller in intestinal than in liver microsomes and that this difference is more prominent for CYP2B11 than for CYP3A12. This also supports the hypothesis that intestinal CYP enzymes may lose their activity during tissue processing and that CYP2B11 may be more vulnerable than CYP3A12. A more in depth exploration of this is warranted but is beyond the scope of the current paper.

Northern Blot data reported in the literature [46] suggest that CYP1A2, but not CYP1A1, is constitutively expressed in the beagle dog liver and that neither CYP1A1 nor CYP1A2 are constitutively expressed in the beagle dog intestine. Thus, CYP1A1 was not expected to be present in the samples studied in the current study. Although this study does not provide direct information on abundance of CYP1A1 or CYP2A13, the observed correlation of EROD activity,

mediated by canine CYP1A1, CYP1A2 and CYP2A13 [27–29], and CYP1A2 abundance in the liver homogenates and microsomes (Fig. 3) is in accordance with the expectation of CYP1A1 absence and also suggests that EROD activity is either not significantly mediated by CYP2A13 in the dog liver or that CYP2A13 activity co-varies with CYP1A2.

In contrast to CYP enzymes, there are no reports of quantitation of individual UGT proteins in the dog available in the literature. Furthermore, gene expression data on dog UGTs is very limited. UGT1A6 and UGT2B31 genes are known to be expressed in the beagle dog liver [35, 36] and the current results confirm that these enzymes are present also as protein. Furthermore, in agreement with current results, UGT1A6 gene expression has been reported to be higher in the liver than in the intestine and approximately 6 fold higher in the colon than in the jejunum whereas the differences between liver and intestinal segments were less prominent for all UGT1As together [47]. Also Haller and co-workers [45] reported that UGT1A6 gene is expressed in both liver and intestine but, in contrast to our protein results, differences between colon and small intestine were not observed.

In further contrast to CYP enzymes, where no enzyme is specific to the intestine, this study identified three UGT1A enzymes (UGTs 1A2, 1A9 and 1A11) showing intestinal expression but low or no abundance in the liver. Correspondingly in human, UGTs 1A7, 1A8 and 1A10 are reported to be present in the intestine but not in the liver (3). This leads to the conclusion that tissue specificity of individual UGT1As in human and dog do not match and therefore the nomenclature used by Li and Wu [34] with the same numbering in animal and human may be misleading since it could be mistakenly interpreted that the enzymes with the same name in dog and human are orthologous pairs. However, although possibly misleading and potentially subject to update in the future, this nomenclature was adopted in the current work for consistency with the currently published literature. A further conclusion, for both dog and human [48], is that *in vitro* metabolism in liver microsomes cannot be used as a predictor for UGT mediated metabolism in the gut wall. This is in contrast to the situation with CYP3A where both liver and gut wall metabolism in human may be predicted from *in vitro* measurements in liver microsomes [49–51]. This approach may be applicable to CYP3A12 mediated metabolism in beagle dog also.

Biological variability of CYP and UGT enzyme abundance

It has been shown that technical variability in sample processing contributes substantially to apparent variability in CYP3A4 abundance measured *in vitro* in human hepatic microsomes (6). Furthermore, prediction of variability in *in vivo*

Table 5 Microsomal Enrichment and Recovery of CYP and UGT Proteins and Activities in Dog Liver Microsomes (DLM)

Microsomal marker						Fold enrichment in DLM (95% confidence interval)	Microsomal recovery % (95% confidence interval)
CYP2C21	A[a]					3.26 (3.01–3.52)	52 (48–56)
UGT1A6	A	B				3.10 (2.87 - 3.35)	50 (46–54)
EROD[b]	A	B				3.10 (2.87 - 3.34)	50 (46–54)
Sum_of_CYPs	A	B	C			2.97 (2.75–3.21)	48 (44–51)
CYP3A12	A	B	C			2.94 (2.72 - 3.18)	47 (44–51)
CYP2D15	A	B	C			2.90 (2.68 - 3.13)	46 (43–50)
CYP2E1	A	B	C			2.88 (2.67–3.11)	46 (43–50)
CYP2B11	A	B	C			2.86 (2.65–3.09)	46 (42–49)
CYP1A2	A	B	C	D		2.78 (2.58–3.01)	45 (41–48)
Sum_of_UGTs		B	C	D	E	2.67 (2.47–2.88)	43 (40–46)
UGT2B31		B	C	D	E	2.65 (2.46–2.86)	43 (40–46)
UGT1A7		B	C	D	E	2.62 (2.42–2.82)	42 (39–45)
UGT1A3		B	C	D	E	2.61 (2.42–2.82)	42 (39–45)
UGT1A1			C	D	E	2.47 (2.29–2.67)	40 (37–43)
CYP3A26			C	D	E	2.45 (2.27–2.65)	39 (36–42)
UGT1A2				D	E	2.35 (2.18–2.53)	38 (35–41)
UGT1A4				D	E	2.30 (2.14–2.49)	37 (34–40)
HFC[c]					E	2.23 (2.06–2.40)	36 (33–38)

[a] The fold enrichment of microsomal markers that are not connected with the same letter are significantly different from each other, $\alpha = 0.05$

[b] EROD = 7-ethoxyresorufin de-ethylation activity

[c] HFC = 7-hydroxy-4-trifluoromethylcoumarin glucuronidation

Table 6 Microsomal Enrichment of CYP and UGT Proteins and Activities in Dog Intestinal Microsomes (DIM)

Microsomal marker	Fold enrichment in DIM (95% confidence interval)	Microsomal recovery %(95% confidence interval)
UGT1A11	2.24 (1.73–2.91)	16 (12–21)
Sum_of_CYPs	2.21 (1.70–2.86)	16 (12–20)
CYP3A12	2.17 (1.68–2.82)	15 (8–31)
CYP2B11	2.14 (1.65–2.77)	15 (12–20)
Sum_of_UGTs	2.11 (1.63–2.73)	15 (11–20)
UGT1A1	2.10 (1.62–2.72)	15 (11–20)
UGT1A2	2.09 (1.61–2.71)	15 (11–19)
UGT1A4	1.87 (1.44–2.42)	15 (11–19)
HFC[a]	1.72 (1.33–2.23)	13 (10–17)
UGT1A6	1.66 (0.88–3.13)	12 (9–16)
UGT1A3	1.54 (1.19–2.00)	11 (8–14)
UGT1A9	1.52 (1.17–1.97)	11 (8–14)
Mida[b]	1.26 (0.93–1.72)	9 (6–13)

[a] HFC = 7-hydroxy-4-trifluoromethylcoumarin glucuronidation

[b] Mida = Midazolam 1'-hydroxylation, activity was below the limit of quantitation in part of the samples

The values for different microsomal markers are not significantly different from each other, $\alpha = 0.05$

drug clearance was improved when only biological variability (CV = 41%) was included. Therefore, in addition to quantitation of CYP and UGT abundances, this study aimed to characterize variability by performing the whole liver tissue processing procedure in triplicate and then analyzing the data to separate technical and biological variability. One caveat here is that the tissue samples represent only a single time point for each donor and so the biological variability estimated is a combination of both intra-individual (*e.g.* due to circadian fluctuation [52]) and inter-individual variability. To separate these two sources of biological variability the sample collection would need to be repeated from the same donors over time, which was not possible due to the destructive nature of tissue harvesting in the current study.

Biological variability in hepatic enzyme abundance was estimated within two dog populations. One population comprised only the 14 donors from the Roche Nutley dog colony and the other included also the 4 additional donors from Covance collected for an earlier study on CYP abundance [24]. The latter population analysis included the assumption that technical variability is similar in both sources of samples. The estimates of biological variability varied between the enzymes and were systematically larger when including donors from both sources. This is not entirely unexpected given the age difference (31–35 months for Roche dogs vs 6–13 months for Covance dogs), environmental differences (including investigational drug history of Roche dogs) and potential genetic differences between the donor populations. However, current data do not allow a meaningful analysis of covariates related to enzyme abundance. Despite the small sample sizes and consequent uncertainty on population variability, it can be speculated that the small biological variability estimates (Table 3, CVs ranging from 14 to 49%) obtained using only the data from Roche dogs may better represent the variability within individual dog colonies maintained for research purposes. Thus, these estimates may be suitable for bottom up prediction of variability in populations typically used for PK experiments in drug development. On the other hand, the estimates obtained using the data from all donors (Table 4, CVs ranging from 29 to 74%) may provide a better estimate of variability in the broader beagle population and may thus be more relevant for predicting PK variability for veterinary purposes. However, further work on bottom-up prediction of drug metabolism in the dog is warranted to support this speculation.

For liver samples, the processing included technical replicates but this was not the case for the intestine where sample preparation was conducted as a single process per segment.

Table 7 Estimates of amount of microsomal protein in beagle dog liver and intestine

Tissue	Geometric Mean (95% Confidence Interval)	
	mg/g tissue	mg/cm tissue
Liver	61[a] (56–66)	NA
Small intestine	6.8[a] (4.2–11.0)	5.9[a] (4.1–8.5)
Colon	0.7[b] (0.2–2.9)	1.4[b] (0.5–4.2)

[a] Overall variability in estimates, shown as 95% confidence interval, represents primarily the technical variability as the 95% confidence intervals for estimates of biological variance included 0. Thus, meaningful estimates of biological variability were not obtained

[b] No technical replicates from colon samples. Thus, it is not possible to separate the technical and biological variability

Thus, estimation of contributions of biological and technical variability in observed intestinal enzyme abundance would have to assume interrelationship of enzyme abundance and contributions of different sources of variability between the intestinal segments. Such analysis was considered to be outside of the scope of current report. However, to enable such follow-up analysis the detailed quantitation results are provided in the supplementary Excel data sheet.

Microsomal Enrichment of CYP and UGT Proteins and Activity

Microsomal enrichment was calculated based on 16 enzyme abundance and 2 metabolic activity markers in liver and on 11 enzyme abundance and 2 activity markers in intestine. There were statistically significant differences between markers in the liver (geometric mean fold enriched of different markers ranging from 2.2 to 3.3, Table 5) whereas the differences did not reach statistical significance in the intestine. Furthermore, microsomal enrichment, and especially the estimated fraction of microsomal protein recovered, tended to be lower in the intestinal than in the liver microsomes. These differences are probably due to the presence of mucus in intestinal lumen which causes aggregation of protein and prevents separation of microsomal protein (*Hatley OJD, Jones C, Galetin A & Rostami-Hodjegan A.* [*Manuscript in preparation*]) and there may also be a contribution due to differences in the microsome preparation protocols used for liver and intestinal samples. While differences in microsomal enrichment of different enzymes suggest that vulnerability to loss during cell fractionation may vary from enzyme to enzyme, the fact that the rank order of the enrichment of different markers was different in the intestine and liver might further suggest that differences are also dependent on tissue or cell fractionation protocol. Therefore, similarly to results reported for microsomal recovery of CYP enzymes in human liver microsomes [25], it cannot be concluded from this study that enzyme specific estimates of the amount of microsomal protein in liver tissue should be used for extrapolating drug metabolism from microsomes to intact tissue. Therefore, overall estimates of microsomal protein per unit tissue were calculated based on the enrichment of the sum of CYPs and the sum of UGTs (Table 7). These estimates for the liver [Geometric mean (95% confidence interval), 61 (56–66) mg/g] are slightly higher than the numbers reported in recent literature (43–59 mg/g) [24, 53, 54] and for the small intestine [Geometric mean (95% confidence interval), 6.8 (4.2–11.0) mg/g] are slightly lower than prior results (13 mg/g) [24]. However, given the technical variability in the estimates, these results can be considered to be generally in agreement with prior publications. In contrast, the current estimate for microsomal protein abundance in the colon [Geometric mean (95% confidence interval), 0.7 (0.2–2.9) mg/g] is substantially lower than the estimate reported earlier (6 mg/g) [24]. Furthermore, it appears that the variability in the results from both liver and intestine was primarily due to technical variability making it impossible to establish meaningful estimates of biological variability in the amount of total microsomal protein in these tissues.

Assumptions involved with absolute quantitation of CYP and UGT proteins

Compared to immunologically based methods for protein quantitation, such as Western Blotting and ELISA, SRM mass spectrometry provides superior selectivity and also the possibility to quantitate several proteins in a single assay. Often, highly homologous proteins, such as members of the UGT1A family, can be separately quantified, which would be challenging or impossible with immunologically based methods. Thus, SRM mass spectrometry is a powerful technology to quantify tissue abundance of proteins relevant for drug pharmacokinetics and several reports of absolute quantitation of ADME relevant proteins *via* SRM have recently emerged [2, 3, 55–58]. However it must be recognized that the assumptions made and consequent sources of error, vary depending on the exact methodology employed [59, 60]. The main assumption of the peptide based absolute quantitation approach used in the current study, where heavy peptide standards are spiked into samples after trypsin digestion, is that the protein digestion yields equimolar amounts of peptides. This assumes complete digestion of proteins to proteotypic tryptic peptides without degradation or any other loss during the process. However, it has been shown that both protein digestion and peptide degradation rates are protein and peptide dependent [57, 59]. Consequently it is not surprising that different peptides for the same protein often report different absolute abundances, an issue which has been dealt with in different ways by different investigators. Some have quantitated only one peptide per protein [61, 62] or have chosen just the highest reporting peptide for estimation of protein concentration even when several peptides have actually been quantified [57, 63]. Others, including our previous study on dog CYPs [24], have taken consensus estimates from multiple peptides [64, 65]. If inefficiency of protein digestion and degradation of native peptides during digestion were the only possible sources of error, it could be argued that the highest abundant proteotypic peptide for a protein is likely to result in the least underestimated absolute protein quantitation even though this would still not confirm an equimolar yield of peptide after digestion. However, additional sources of error in peptide quantitation are possible including variation in the actual concentration of spiked in heavy peptides due to inaccuracies in initial quantitation and unknown losses between initial characterization and actual use. Therefore, we decided to report consensus estimates derived using linear mixed effects modeling of data from multiple proteotypic peptides. For

completeness and transparency, we have also reported results based on individual peptides in the supplementary data files. Overall, the highest and lowest abundant peptides of each protein were within 3 fold of each other although CYP2E1 was a notable exception with one of the peptides reporting approximately 6 fold higher concentrations than the other two. The uncertainty in absolute protein abundances due to differences in concentration reported by different proteotypic peptides applies only to the absolute values reported for any given protein. Sample to sample comparisons for the same protein, and thus estimates of biological variability, are not affected by the same uncertainty. It should also be noted that the similarity of the CYP abundance results for the 4 liver and 4 intestinal samples measured in the current and the previous [24] studies support the reproducibility of the results (data supplement, Figure 7-S and Table 1-S). Furthermore, the effective utilization of quantitative protein expression data for IVIVE of enzyme activity does not necessarily require accurate absolute enzyme abundance quantitation but, rather, relies on precise relative enzyme abundance in the tissues *versus* the *in vitro* assay (s). Moreover, it should be acknowledged that successful IVIVE of drug metabolism often requires additional empirical scaling factors to correct for differences in specific enzyme activity in different experimental platforms [66, 67]. Consequently, the absolute abundances reported, even if biased, alongside sufficiently detailed description of the methodology applied, should enable bridging of the data generated in different studies and, thus, provide a reasonable starting point for establishment of useful IVIVE scaling factors.

A degree of caution is also needed concerning the identity of the proteins reported since current databases of beagle dog genome and proteome are not complete, leaving the possibility that the selected peptides are not proteotypic. This is especially the case with UGT2B31 as although it is the only known member of the UGT2B family in the dog, information for other species shows the presence of several hepatic UGT2B isoforms [56, 57, 68, 69] and it may be that this is also the case in dog. Thus, although it cannot be ruled out that the abundance assigned to UGT2B31 in the current study actually represents more than one UGT2B isoform, our use of more than one proteotypic peptide per protein whenever possible and the correlation in signals throughout the samples support that the peptides do truly originate from the same protein (or proteins).

CONCLUSION

In conclusion, this work provides insights on the abundances of drug metabolizing enzymes in the beagle dog liver and intestine. In addition to differences in expression levels between liver and intestine, the study has also highlighted differential tissue specificity for UGT1As in dog and human. Generated proteomic data will serve as a basis for *in vitro in vivo* extrapolation of CYP and UGT mediated metabolism in these tissues also allowing bottom up prediction of variability in a beagle dog population. Further research is required to demonstrate the utility of physiologically based pharmacokinetics models of beagle dog including these data.

ACKNOWLEDGMENTS AND DISCLOSURES

This work was funded by Roche Postdoc Fellowship (RPF) program. The authors gratefully acknowledge: Zheng Yang (Bristol-Myers Squibb) for kind offering of labs and organisation of placement for intestinal microsome preparation; Mary Obermeier (Bristol-Myers Squibb) for assistance in the lab during intestinal microsome preparation; Laura Singer, Heather Martin, David Wellington and Claudia Suenderhauf (all Roche) for contributions on dog tissue collection and shipment; Martin Ebeling and Marco Berrera (Roche) for compiling the dog protein database; Peter Jakob (Roche) for sample preparation for MS experiments; Hannele Jaatinen, Pirjo Hänninen and Virpi Koponen (all University of Eastern Finland) for support in liver sample processing and characterization.

Supporting Information Supplementary data is provided in data supplements available in electronic form: Illustrative figures of CYP and UGT enzyme abundance and activity, SRM assay parameters and study-to-study comparison of CYP quantitation results, and CYP and UGT abundance in individual samples.

REFERENCES

1. Sakamoto A, Matsumaru T, Ishiguro N, *et al.* Reliability and robustness of simultaneous absolute quantification of drug transporters, cytochrome P450 enzymes, and Udp-glucuronosyltransferases in human liver tissue by multiplexed MRM/selected reaction monitoring mode tandem mass spectrometry with nano-liquid chromatography. J Pharm Sci. 2011;100:4037–43.
2. Miliotis T, Ali L, Palm JE, *et al.* Development of a Highly Sensitive Method using LC-MRM to Quantify Membrane P-glycoprotein in Biological Matrices and Relationship to Transport Function. Drug Metab Dispos. 2011;39:2440–9.
3. Harbourt DE, Fallon JK, Ito S, *et al.* Quantification of human uridine-diphosphate glucuronosyl transferase 1A isoforms in liver, intestine, and kidney using nanobore liquid chromatography–tandem mass spectrometry. Anal Chem. 2011;84:98–105.
4. Harwood MD, Neuhoff S, Carlson GL, Warhurst G, Rostami-Hodjegan A. Absolute abundance and function of intestinal drug transporters: a prerequisite for fully mechanistic *in vitro-in vivo* extrapolation of oral drug absorption. Biopharm Drug Dispos. 2013;34:2–28.
5. Rostami-Hodjegan A, Tucker GT. Simulation and prediction of *in vivo* drug metabolism in human populations from *in vitro* data. Nat Rev. 2007;6:140–8.
6. Cubitt HE, Yeo KR, Howgate EM, Rostami-Hodjegan A, Barter ZE. Sources of interindividual variability in IVIVE of clearance: an

investigation into the prediction of benzodiazepine clearance using a mechanistic population-based pharmacokinetic model. Xenobiotica. 2011;41:623–38.
7. Barter ZE, Tucker GT, Rowland-Yeo K. Differences in cytochrome p450-mediated pharmacokinetics between Chinese and Caucasian populations predicted by mechanistic physiologically based pharmacokinetic modelling. Clin Pharmacokinet. 2013;52:1085–100.
8. Uchida Y, Ohtsuki S, Kamiie J, Terasaki T. Blood–brain barrier (BBB) pharmacoproteomics: reconstruction of *in vivo* brain distribution of 11 P-glycoprotein substrates based on the BBB transporter protein concentration, *in vitro* intrinsic transport activity, and unbound fraction in plasma and brain in mice. J Pharmacol Exp Ther. 2011;339:579–88.
9. Heikkinen AT, Fowler S, Gray L, *et al. In vitro* to *in vivo* extrapolation and physiologically based modeling of cytochrome p450 mediated metabolism in beagle dog gut wall and liver. Mol Pharm. 2013;10:1388–99.
10. Prasad B, Evers R, Gupta A, *et al.* Interindividual variability in hepatic organic anion-transporting polypeptides and P-glycoprotein (ABCB1) protein expression: quantification by liquid chromatography tandem mass spectroscopy and influence of genotype, age, and sex. Drug Metab Dispos. 2014;42:78–88.
11. Jones HM, Parrott N, Jorga K, Lave T. A novel strategy for physiologically based predictions of human pharmacokinetics. Clin Pharmacokinet. 2006;45:511–42.
12. Rowland M, Peck C, Tucker G. Physiologically-Based Pharmacokinetics in Drug Development and Regulatory Science. Annu Rev Pharmacol Toxicol. 2011;51:45–73.
13. Garren KW, Rahim S, Marsh K, Morris JB. Bioavailability of generic ritonavir and Lopinavir/ritonavir tablet products in a dog model. J Pharm Sci. 2010;99:626–31.
14. Paulson SK, Vaughn MB, Jessen SM, *et al.* Pharmacokinetics of celecoxib after oral administration in dogs and humans: effect of food and site of absorption. J Pharmacol Exp Ther. 2001;297:638–45.
15. Xia B, Heimbach T, Lin TH, *et al.* Utility of physiologically based modeling and preclinical *in vitro*/*in vivo* data to mitigate positive food effect in a BCS class 2 compound. AAPS PharmSciTech. 2013;14:1255–66.
16. Kuentz M, Nick S, Parrott N, Röthlisberger D. A strategy for preclinical formulation development using GastroPlus™ as pharmacokinetic simulation tool and a statistical screening design applied to a dog study. Eur J Pharm Sci. 2006;27:91–9.
17. Kesisoglou F. Use of preclinical dog studies and absorption modeling to facilitate late stage formulation bridging for a BCS II drug candidate. AAPS PharmSciTech. 2013.
18. Dressman JB. Comparison of canine and human gastrointestinal physiology. Pharm Res. 1986;3:123–31.
19. Lui CY, Amidon GL, Berardi RR, *et al.* Comparison of gastrointestinal pH in dogs and humans: implications on the use of the beagle dog as a model for oral absorption in humans. J Pharm Sci. 1986;75:271–4.
20. Martinez MN, Papich MG. Factors influencing the gastric residence of dosage forms in dogs. J Pharm Sci. 2009;98:844–60.
21. Soars MG, Riley RJ, Findlay KAB, Coffey MJ, Burchell B. Evidence for significant differences in microsomal drug glucuronidation by canine and human liver and kidney. Drug Metab Dispos. 2001;29:121–6.
22. Prueksaritanont T, Gorham LM, Hochman JH, Tran LO, Vyas KP. Comparative studies of drug-metabolizing enzymes in dog, monkey, and human small intestines, and in caco-2 cells. Drug Metab Dispos. 1996;24:634–42.
23. Arndt M, Chokshi H, Tang K, *et al.* Dissolution media simulating the proximal canine gastrointestinal tract in the fasted state. Eur J Pharm Biopharm. 2013;84:633–41.
24. Heikkinen AT, Friedlein A, Lamerz J, *et al.* Mass spectrometry-based quantification of CYP enzymes to establish *in vitro* - *in vivo* scaling factors for intestinal and hepatic metabolism in beagle Dog. Pharm Res. 2012;29:1832–42.
25. Hakooz N, Ito K, Rawden H, *et al.* Determination of a human hepatic microsomal scaling factor for predicting *in vivo* drug clearance. Pharm Res. 2006;23:533–9.
26. Martinez MN, Antonovic L, Court M, *et al.* Challenges in exploring the cytochrome P450 system as a source of variation in canine drug pharmacokinetics. Drug Metab Rev. 2013;45:218–30.
27. Shou M, Norcross R, Sandig G, *et al.* Substrate specificity and kinetic properties of seven heterologously expressed dog cytochromes p450. Drug Metab Dispos. 2003;31:1161–9.
28. Mise M, Yadera S, Matsuda M, *et al.* Polymorphic expression of CYP1A2 leading to interindividual variability in metabolism of a novel benzodiazepine receptor partial inverse agonist in dogs. Drug Metab Dispos. 2004;32:240–5.
29. Zhou D, Linnenbach AJ, Liu R, *et al.* Expression and characterization of dog cytochrome P450 2A13 and 2A25 in baculovirus-infected insect cells. Drug Metab Dispos. 2010;38:1015–8.
30. Locuson CW, Ethell BT, Voice M, Lee D, Feenstra KL. Evaluation of escherichia coli membrane preparations of canine CYP1A1, 2B11, 2C21, 2C41, 2D15, 3A12, and 3A26 with coexpressed canine cytochrome P450 reductase. Drug Metab Dispos. 2009;37:457–61.
31. Rahikainen T, Häkkinen MR, Finel M, Pasanen M, Juvonen RO. A high throughput assay for the glucuronidation of 7-hydroxy-4-trifluoromethylcoumarin by recombinant human UDP-glucuronosyltransferases and liver microsomes. Xenobiotica. 2013.
32. Tenmizu D, Endo Y, Noguchi K, Kamimura H. Identification of the novel canine CYP1A2 1117 C>T SNP causing protein deletion. Xenobiotica. 2004;34:835–46.
33. Roussel F, Duignan DB, Lawton MP, *et al.* Expression and characterization of canine cytochrome P450 2D15. Arch Biochem Biophys. 1998;357:27–36.
34. Li C, Wu Q. Adaptive evolution of multiple-variable exons and structural diversity of drug-metabolizing enzymes. BMC Evol Biol. 2007;7:69.
35. Soars MG, Fettes M, O'Sullivan AC, *et al.* Cloning and characterisation of the first drug-metabolising canine UDP-glucuronosyltransferase of the 2B subfamily. Biochem Pharmacol. 2003;65:1251–9.
36. Soars MG, Smith DJ, Riley RJ, Burchell B. Cloning and characterization of a canine UDP-glucuronosyltransferase. Arch Biochem Biophys. 2001;391:218–24.
37. MacLean B, Tomazela DM, Shulman N, *et al.* Skyline: an open source document editor for creating and analyzing targeted proteomics experiments. Bioinformatics. 2010;26:966–8.
38. Röst H, Malmström L, Aebersold R. A computational tool to detect and avoid redundancy in selected reaction monitoring. Mol Cell Proteomics : MCP. 2012;11:540–9.
39. Mise M, Hashizume T, Matsumoto S, Terauchi Y, Fujii T. Identification of non-functional allelic variant of CYP1A2 in dogs. Pharmacogenetics. 2004;14:769–73.
40. Eguchi K, Nishibe Y, Baba T, Ohno K. Quantitation of cytochrome P450 enzymes (CYP1A1/2, 2B11, 2C21 and 3A12) in dog liver microsomes by enzyme-linked immunosorbent assay. Xenobiotica. 1996;26:755–63.
41. Nishibe Y, Wakabayashi M, Harauchi T, Ohno K. Characterization of cytochrome P450 (CYP3A12) induction by rifampicin in dog liver. Xenobiotica. 1998;28:549–57.
42. Kyokawa Y, Nishibe Y, Wakabayashi M, *et al.* Induction of intestinal cytochrome P450 (CYP3A) by rifampicin in beagle dogs. Chem Biol Interact. 2001;134:291–305.
43. Sakamoto K, Kirita S, Baba T, *et al.* A new cytochrome P450 form belonging to the CYP2D in dog liver microsomes: purification, cDNA cloning, and enzyme characterization. Arch Biochem Biophys. 1995;319:372–82.
44. Mealey KL, Jabbes M, Spencer E, Akey JM. Differential expression of CYP3A12 and CYP3A26 mRNAs in canine liver and intestine. Xenobiotica. 2008;38:1305–12.

45. Haller S, Schuler F, Lazic SE, *et al.* Expression profiles of metabolic enzymes and drug transporters in the liver and along the intestine of beagle dogs. Drug Metab Dispos. 2012;40:1603–11.
46. Uchida T, Komori M, Kitada M, Kamataki T. Isolation of cDNAs coding for three different forms of liver microsomal cytochrome P-450 from polychlorinated biphenyl-treated beagle dogs. Mol Pharmacol. 1990;38:644–51.
47. Bock KW, Bock KW, Bock-Hennig BS, *et al.* Tissue-specific regulation of canine intestinal and hepatic phenol and morphine UDP-glucuronosyltransferases by β-naphthoflavone in comparison with humans. Biochem Pharmacol. 2002;63:1683–90.
48. Nishimuta H, Sato K, Yabuki M, Komuro S. Prediction of the intestinal first-pass metabolism of CYP3A and UGT substrates in humans from *in vitro* data. Drug Metab Pharmacokinet. 2011.
49. Gertz M, Harrison A, Houston JB, Galetin A. Prediction of human intestinal first-pass metabolism of 25 CYP3A substrates from *in vitro* clearance and permeability data. Drug Metab Dispos. 2010;38:1147–58.
50. Heikkinen AT, Baneyx G, Caruso A, Parrott N. Application of PBPK modeling to predict human intestinal metabolism of CYP3A substrates – an evaluation and case study using GastroPlus™. Eur J Pharm Sci. 2012;47:375–86.
51. Galetin A, Houston JB. Intestinal and hepatic metabolic activity of five cytochrome P450 enzymes: impact on prediction of first-pass metabolism. J Pharmacol Exp Ther. 2006;318:1220–9.
52. Froy O. Cytochrome P450 and the biological clock in mammals. Curr Drug Metab. 2009;10:104–15.
53. Smith R, Jones RD, Ballard PG, Griffiths HH. Determination of microsome and hepatocyte scaling factors for *in vitro/in vivo* extrapolation in the rat and dog. Xenobiotica. 2008;38:1386–98.
54. Bäärnhielm C, Dahlbäck H, Skånberg I. *In vivo* pharmacokinetics of felodipine predicted from *in vitro* studies in rat, dog and man. Acta Pharmacol Toxicol. 1986;59:113–22.
55. Kamiie J, Ohtsuki S, Iwase R, *et al.* Quantitative atlas of membrane transporter proteins: development and application of a highly sensitive simultaneous LC/MS/MS method combined with novel in-silico peptide selection criteria. Pharm Res. 2008;25:1469–83.
56. Ohtsuki S, Schaefer O, Kawakami H, *et al.* Simultaneous absolute protein quantification of transporters, cytochromes P450, and UDP-glucuronosyltransferases as a novel approach for the characterization of individual human liver: comparison with mRNA levels and activities. Drug Metab Dispos. 2012;40:83–92.
57. Fallon JK, Neubert H, Hyland R, Goosen TC, Smith PC. Targeted quantitative proteomics for the analysis of 14 UGT1As and -2Bs in human liver using NanoUPLC-MS/MS with selected reaction monitoring. J Proteome Res. 2013;12:4402–13.
58. Achour B, Russell MR, Barber J, Rostami-Hodjegan A. Simultaneous quantification of the abundance of several cytochrome P450 and uridine 5'-diphospho-glucuronosyltransferase enzymes in human liver microsomes using multiplexed targeted proteomics. Drug Metab Dispos. 2014;42:500–10.
59. Shuford CM, Sederoff RR, Chiang VL, Muddiman DC. Peptide production and decay rates affect the quantitative accuracy of protein cleavage isotope dilution mass spectrometry (PC-IDMS). Mol Cell Proteomics. 2012;11:814–23.
60. Lange V, Picotti P, Domon B, Aebersold R. Selected reaction monitoring for quantitative proteomics: a tutorial. Mol Syst Biol. 2008;4:222.
61. Gerber SA, Rush J, Stemman O, Kirschner MW, Gygi SP. Absolute quantification of proteins and phosphoproteins from cell lysates by tandem MS. Proc Natl Acad Sci U S A. 2003;100:6940–5.
62. Kawakami H, Ohtsuki S, Kamiie J, *et al.* Simultaneous absolute quantification of 11 cytochrome P450 isoforms in human liver microsomes by liquid chromatography tandem mass spectrometry with in silico target peptide selection. J Pharm Sci. 2010;100:341–52.
63. Percy AJ, Chambers AG, Yang J, Hardie DB, Borchers C.H. Advances in multiplexed MRM-based protein biomarker quantitation toward clinical utility. Biochim Biophys Acta .2013.
64. Campbell J, Rezai T, Prakash A, *et al.* Evaluation of absolute peptide quantitation strategies using selected reaction monitoring. Proteomics. 2011;11:1148–52.
65. Langenfeld E, Zanger UM, Jung K, Meyer HE, Marcus K. Mass spectrometry-based absolute quantification of microsomal cytochrome P450 2D6 in human liver. Proteomics. 2009;9:2313–23.
66. Proctor NJ, Tucker GT, Rostami-Hodjegan A. Predicting drug clearance from recombinantly expressed CYPs: intersystem extrapolation factors. Xenobiotica. 2004;34:151–78.
67. Chen Y, Liu L, Nguyen K, Fretland AJ. Utility of intersystem extrapolation factors in early reaction phenotyping and the quantitative extrapolation of human liver microsomal intrinsic clearance using recombinant cytochromes P450. Drug Metab Dispos. 2011;39:373–82.
68. Ohno S, Nakajin S. Determination of mRNA expression of human UDP-glucuronosyltransferases and application for localization in various human tissues by real-time reverse transcriptase-polymerase chain reaction. Drug Metab Dispos. 2009;37:32–40.
69. Meech R, Miners JO, Lewis BC, Mackenzie PI. The glycosidation of xenobiotics and endogenous compounds: versatility and redundancy in the UDP glycosyltransferase superfamily. Pharmacol Ther. 2012;134:200–18.